Orientation of tendons in vivo with active and passive knee muscles

Aalbersberg-van Berkel, S.; Kingma, I.; Ronsky, J.L.; Frayne, R.; van Dieen, J.H.

published in
Journal of Biomechanics
2005

DOI (link to publisher)
10.1016/j.jbiomech.2004.09.003

ELSEVIER

Journal of Biomechanics 38 (2005) 1780–1788

JOURNAL OF BIOMECHANICS

www.elsevier.com/locate/jbiomech
www.JBiomech.com

Orientation of tendons in vivo with active and passive knee muscles

Sietske Aalbersberg[a], Idsart Kingma[a,*], Janet L. Ronsky[b], Richard Frayne[c], Jaap H. van Dieën[a]

[a]*Institute for Fundamental and Clinical Human Movement Sciences, Faculty of Human Movement Sciences, Vrije Universiteit, Van der Boechorststraat 9, 1081 BT Amsterdam, The Netherlands*
[b]*Department of Mechanical and Manufacturing Engineering, University of Calgary, Calgary, Canada*
[c]*Departments of Radiology and Clinical Neurosciences, Seaman Family MR Research Centre, Foothills Medical Centre/University of Calgary, Calgary, Canada*

Accepted 9 September 2004

Abstract

Tendon orientations in knee models are often taken from cadaver studies. The aim of this study was to investigate the effect of muscle activation on tendon orientation in vivo. Magnetic resonance imaging (MRI) images of the knee were made during relaxation and isometric knee extensions and flexions with 0°, 15° and 30° of knee joint flexion. For six tendons, the orientation angles in sagittal and frontal plane were calculated. In the sagittal plane, muscle activation pulled the patellar tendon to a more vertical orientation and the semitendinosus and sartorius tendons to a more posterior orientation. In the frontal plane, the semitendinosus had a less lateral orientation, the biceps femoris a more medial orientation and the patellar tendon less medial orientation in loaded compared to unloaded conditions. The knee joint angle also influenced the tendon orientations. In the sagittal plane, the patellar tendon had a more anterior orientation near full extension and the biceps femoris had an anterior orientation with 0° and 15° flexions and neutral with 30° flexions. Within 0° to 30° of flexion, the biceps femoris cannot produce a posterior shear force and the anterior angle of the patellar tendon is always larger than the hamstring tendons. Therefore, co-contraction of the hamstring and quadriceps is unlikely to reduce anterior shear forces in knee angles up to 30°. Finally, inter-individual variation in tendon angles was large. This suggests that the amount of shear force produced and the potential to counteract shear forces by co-contraction is subject-specific.

Keywords: Knee; Tendon orientation; Magnetic resonance imaging; Muscle activation; Shear force

1. Introduction

Shear forces in the knee joint can cause injuries (such as anterior cruciate ligament ruptures). The resultant shear forces in the joint depend on the magnitude and direction of external forces and muscle forces. Muscle forces are difficult to measure and therefore usually predicted from biomechanical models. However, the predicted shear force at the joint is sensitive to assumptions regarding the direction of muscle forces.

So far, most knee models (e.g. Blankevoort and Huiskes, 1996; Lloyd and Buchanan, 1996; O'Connor, 1993; Shelburne and Pandy, 1997; Zavatsky and O'Connor, 1992) have used tendon orientation and moment arm data obtained from cadaver studies (Brand et al., 1982; Buford et al., 1997; Herzog and Read, 1993; Spoor and van Leeuwen, 1992). However, the orientation of the tendons and thus the direction of the muscle force might be influenced by muscle activation. Magnetic resonance imaging (MRI) provides the possibility

Abbreviations: ACL; Anterior cruciate ligament; BF; Biceps femoris; GR; Gracilis; MRI; Magnetic resonance imaging; PT; Patellar tendon; SM; Semimembranosus; SR; Sartorius; ST; Semitendinosus; TB; Tibia.

*Corresponding author. Tel.: +31 20 4448492; fax: +31 20 4448529.
E-mail address: i_kingma@fbw.vu.nl (I. Kingma).

0021-9290/$ - see front matter © 2004 Elsevier Ltd. All rights reserved.
doi:10.1016/j.jbiomech.2004.09.003

of examining muscle tendons in vivo. Until recently, it was not possible to examine muscle tendons while the muscles were activated with MRI, because of lengthy data acquisition times (Wretenberg et al., 1996). However, MRI technology has been greatly improved in recent years reducing scanning time significantly. The main purpose of this study was to test the hypothesis that muscle activation will change the orientation of tendons around the knee. A secondary aim was to provide data for 3D biomechanical modeling of the muscles around the knee. Since the knee joint angle also affects tendon orientation (Nisell et al., 1986), the effect of muscle activation was studied at three knee joint angles (0°, 15° and 30°). Larger flexion angles were not possible due to the available MR scanner bore size.

2. Method

2.1. Subjects

Five male and three female subjects participated in this study (Table 1). The right knee of all subjects was scanned using MRI. None of the subjects reported previous injury to or complaints of the knee. The protocol was approved by the conjoint Ethics Board of the University of Calgary and Calgary Health Region. All subjects signed an informed consent before MRI.

2.2. MRI protocol

A 3 T MR scanner (Signa; GE Medical Systems, Waukesha, WI) was used for this study. All imaging was performed using the body coil. Because literature showed a wide range of MRI parameters used to image tendons (e.g. T1-weighted spin-echo: Munshi et al., 2003, T2-weighted spin-echo: El-Dieb et al., 2002; Jaramillo et al., 1994; Major and Helms, 2002, proton density: Jaramillo et al., 1994), a pilot study was done to find the best set-up for knee tendon imaging with the 3 T MRI. The best images were obtained using T1-weighted oblique axial imaging (TR 616 s, TE 14 s, FOV 16 cm, slice thickness 3 mm, matrix 256×192, pixel dim. 0.31×0.31 mm, Echo number 1). T1-weighted images were made in the plane perpendicular to the long axis of the body coil and approximately parallel to the tibia plateau. Thirty-five 3-mm slices were acquired starting at the center of the patella and ending just below the tuberositas tibiae. Each acquisition required either 4.12 or 4.54 min of scanning, depending on the obliquity of the acquired image plane.

2.3. Experimental set-up

Scanning took place with and without activation of the muscles around the knee. The subjects were asked to perform isometric knee extensions and flexions during the scanning. A custom-built loading device (Ronsky, 1994) was modified to allow loading in flexion and extension direction (Fig. 1). A support was placed under the upper leg and the leg was strapped to the board. The foot was placed between two wooden bars, preventing internal and external rotation of the leg. The heel was hung in a rubber band that supported the foot. A non-elastic band was placed over the ventral side of the lower leg near the ankle joint. For isometric knee extensions, the subject was asked to lift the lower leg until the band over the ventral side of the ankle became taut, without really pushing against it. At this point, the foot was still partly resting in the rubber band. Therefore, the subject lifted only a part of the weight of the lower leg. The entire weight would have been too large to maintain for the duration of the task. For isometric flexions, the subject was asked to push the heel downward, thereby stretching the rubber band, until the heel just touched the wooden frame. The change of length of the rubber band (in both the extension and the flexion loading) was approximately 17.5 mm, corresponding to a load change of 8.7 N. We assumed that the force on the ventral non-elastic band in extension, and on the wooden frame in flexion could be neglected. By multiplying the 8.7 N by the moment arm of the load, the flexion and extension

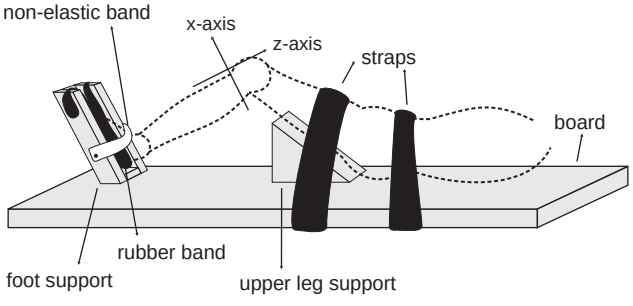

Fig. 1. Schematic overview of the loading device used in the MRI.

Table 1
Subject characteristics (average ± standard deviation)

	Sex (m/f)	Age (yr)	Height (cm)	Weight (kg)	Leg length (cm)	Lower leg length (cm)	Knee width (cm)
Subjects	5/3	26.1 ± 5.3	171.4 ± 3.7	68.9 ± 4.9	83.5 ± 4.9	44.9 ± 2.2	9.8 ± 0.5

loading was calculated to be on average 4.6 Nm (±0.2 Nm).

The subjects performed the isometric knee flexion and extension contraction at three knee angles (0°, 15° and 30°). The order of the knee angles was randomized. With each joint angle, the force direction was systematically varied with the unloaded scan always in between the flexion and extension condition. The subject was taken out of the scanner when the knee angle had to be changed. This ensured a resting period of at least 5 min between two loaded conditions.

2.4. Data analysis

The following muscle tendons were analyzed: patellar tendon (PT), gracilis (GR), sartorius (SR), semimembranosus (SM), semitendinosus (ST), and biceps femoris (BF). An optimization procedure (least squares fit) was used to correct any leg movement during the measurement. The result was visually checked and further corrected when needed. The bones and muscle tendons were identified and colored in each image (Fig. 3a; sliceOmatic, Tomovision, Virtual Magic Inc., Montreal, Canada). Contour data points of the bones and tendons were transferred to Matlab (The Mathworks Inc., Natick, MA, United States). The centroid of the contour of the tendons was calculated in each slice (Crisco and McGovern, 1998), and a second-order polynomial function was fitted through these centroids to form a centroid curve (Fig. 2, Koolstra et al., 1989). This centroid curve represents the line of action of the tendon. The direction of the polynomial was calculated at the point where it crossed the tibia (TB) plateau level, except for the BF where the level was taken 10 mm below the TB plateau to avoid the small part of the tendon that attaches to the tibia edge. It was not possible to locate the exact point of insertion.

With the aid of the loading device, the lower leg was aligned with the long axis of the MRI coil. The sagittal plane of the MRI coordinate system can thus be used as the sagittal plane of the local tibia coordinate system. Rotational alignment of the leg was visually checked by superimposing the tibia contour slices of all trials of a subject over the tibia contour slices of the extension trial at 0° of knee joint flexion of the same subject. When necessary, leg rotation was manually corrected. To complete the local coordinate system, an anterior-posterior line through the center of the medial tibial plateau was obtained through the following steps. First, a vertical line was drawn through the center of the femur in the mid-sagittal plane. In the frontal plane through this line, the center of the medial tibia plateau was selected. The sagittal slice selected in this way was averaged with five sagittal slices to the left and right of this slice. Then, a spline-function was applied in proximal-distal direction of this 'averaged' slice to improve the spatial resolution of the image in this direction. Second, the tibia was identified on this image by automatically finding the gray-scale values above a fixed threshold level. Third, the edge of the tibia plateau was approximated by a sixth-order polynomial function, and the anterior and posterior top of the plateau were identified (Fig. 3b). Finally, the tops were used to construct a line and this line represented the *x*-axis (anterior-posterior) of the local coordinate system (Fig. 4). The origin of the axes system was set on the polynomial of the PT tendon, 10 mm below the tibia plateau.

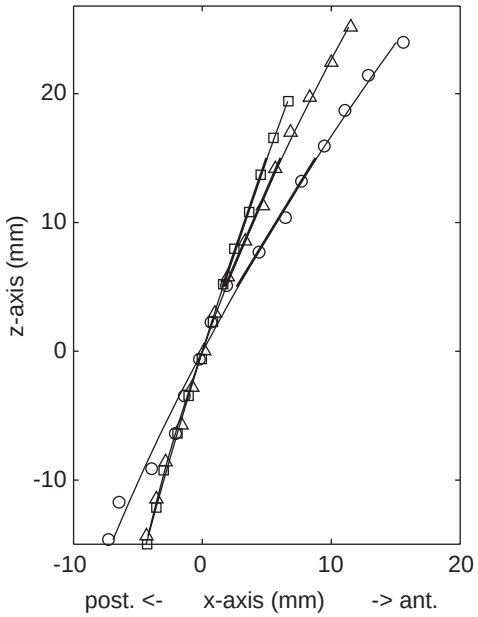

Fig. 2. Typical example of a second order polynomial function fitted through the centroids of a tendon. The data points are the centroids of the PT tendon of subject 6 in the sagittal plane. The knee joint angle was 15°, square stands for extension, triangle stands for unloaded and circle stands for flexion trial. Bold lines are the tangent lines at z = 10 mm, post. = posterior, ant. = anterior.

2.5. Statistics

In total six out of 72 trials were omitted due to subject claustrophobia or limited scanning time. One trial was excluded because of movement artifacts. For each tendon, a univariate ANOVA with subject as random factor was performed using the tendon angles as dependent variables. The independent variables were knee joint angle (three levels) and loading direction (three levels). Due to limitations in degrees of freedom, interactions with subject were not taken into account. The significance level (*p*-value) was set at 0.05 and post-hoc tests (Bonferroni) were performed when the effects of joint angle or loading direction were significant.

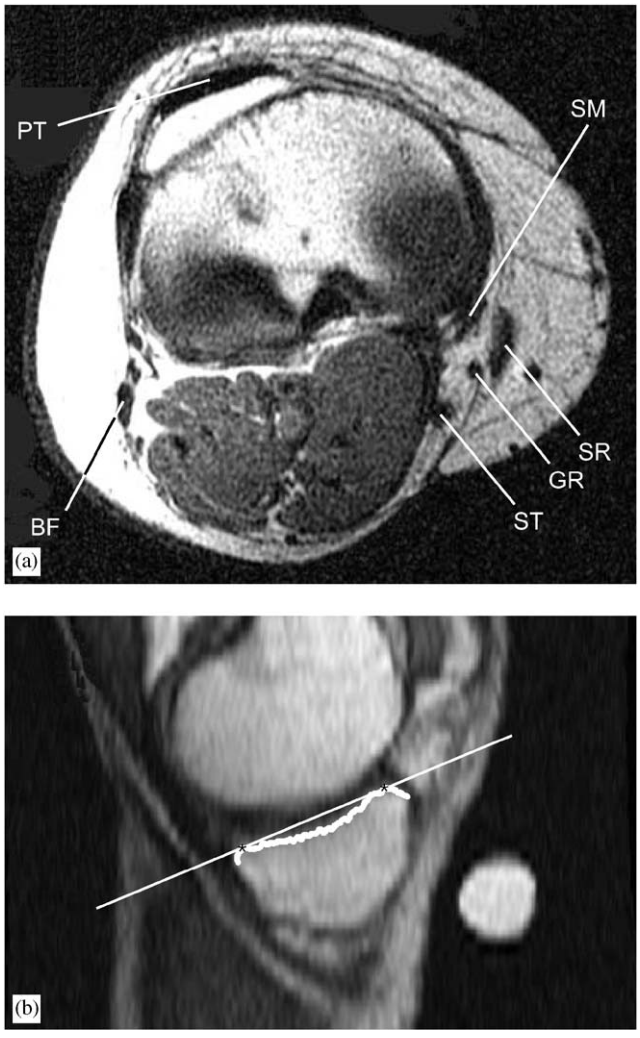

Fig. 3. (a) Typical example of an axial image (subject 6, unloaded, 15° knee flexion). (b) Boundary of gray-values (white dots) of the tibia plateau above the threshold and the line that represent the direction of the tibia plateau. BF = biceps femoris, GR = gracilis, PT = patella, SM = semimembranosus, ST = semitendinosus tendon.

3. Results

For all conditions, the coordinates of the direction vectors of the tendons and the points where these vectors cross the tibia plateau are given in Table 2. For easier interpretation of the data, the vectors are recalculated to angles in the sagittal and frontal plane. The results are presented in Table 3 and the corresponding ANOVA results are given in Table 4. The between-subject variations in tendon angles were large, as can be seen from the standard deviations (Table 3), which are often larger than the within-subject variations due to knee joint angle and loading of the tendon (Table 5).

No interaction effects were found between knee joint angle and loading, except for the SR tendon in the frontal plane. The tendon angles (Table 3) are the angles between the tendon directions and a line perpendicular to the tibia plateau (Fig. 4). If this angle is positive in the

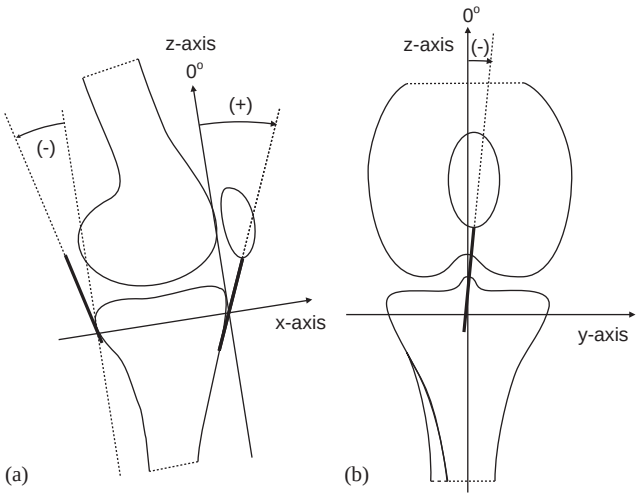

Fig. 4. Tibia coordinate system and angle definition in the sagittal (a) and frontal (b) plane. The origin of the coordinate system is located on the PT tendon, 10 mm below the tibia plateau.

sagittal plane, the tendon produces an anterior shear force on the tibia. The angle of the PT, ST, GR and SR tendons in the sagittal plane (Table 3) were significantly influenced by the load direction (Table 4). A visualization of the effects of loading on three tendons is given in Fig. 5c and d. The PT tendon had a 3.6° (±5.6°) less anterior orientation in extension compared to unloaded conditions. The ST, GR and SR tendons had a more posterior orientation (4.9°±5.1°, 4.8°±7.7° and 7.7°±11.1°, respectively) in flexion compared to extension. In the frontal plane, the PT, ST and BF tendons were significantly affected by the loading direction (Table 4). The PT tendon had a 6.2° (±5.4°) less medial orientation in extension compared to unloaded conditions. The ST tendon had a 1.9° (±2.5°) less lateral orientation in flexion compared to extension. Finally, the tendon of the BF had a 4.3° (±4.3°) more medial orientation in flexion compared to unloaded conditions.

The knee joint angle had a significant influence on the direction of the PT and BF in the sagittal plane (Table 4). A visualization of the effects of knee angle on three tendons is given in Fig. 5a and b. The PT angle was significantly smaller (4.7°±5.1°) in 30° compared to 0° of knee flexion. The BF tendon had an anterior direction in 0° and 15° and changed to an orientation almost perpendicular to the tibia plateau in 30° of knee flexion. In the frontal plane, the PT was significantly influenced by the knee flexion angle. The angle between the tibia plateau and the PT was medially directed at 0° of knee flexion and became 6.3° (±4.8°) or 7.9° (±5.5°) less medially directed when the knee was flexed to 15° or 30° of knee flexion, respectively. The SM and SR tendon were also significantly affected by the knee angle and both had an orientation more perpendicular (with 4.8°±7.3° and 1.8°±6.0°, respectively) to the tibia plateau in 30° compared to 0°.

Table 2
Direction vectors and location vectors of the tendons in the tibia coordinate system

Tendon	Condition		Direction vector						Location vector			
			x		*y*		*z*		*x*		*y*	
			Mean	SD	Mean	SD	Mean	SD	Mean	SD	Mean	SD
PT	0°	ext	0.49	0.05	0.17	0.07	0.85	0.04	5.91	0.83	2.34	0.97
		unl	0.52	0.08	0.31	0.08	0.79	0.07	6.46	1.59	3.98	1.08
		fl	0.51	0.11	0.20	0.09	0.82	0.08	5.68	1.60	2.55	1.07
	15°	ext	0.43	0.05	0.14	0.10	0.89	0.03	4.86	0.83	1.56	1.14
		unl	0.51	0.11	0.18	0.09	0.83	0.07	5.94	1.82	2.19	0.99
		fl	0.52	0.07	0.13	0.06	0.84	0.05	5.65	1.01	1.73	0.80
	30°	ext	0.43	0.05	0.10	0.08	0.89	0.02	4.77	0.75	1.28	0.69
		unl	0.46	0.09	0.16	0.07	0.87	0.05	5.14	1.15	2.10	0.70
		fl	0.46	0.10	0.12	0.09	0.87	0.06	4.97	1.46	1.64	0.89
SM	0°	ext	−0.24	0.16	−0.16	0.11	0.94	0.06	−66.46	5.37	31.57	5.74
		unl	−0.29	0.09	−0.07	0.11	0.95	0.04	−65.90	7.07	30.88	6.81
		fl	−0.29	0.09	−0.11	0.17	0.93	0.05	−56.94	6.75	36.75	5.80
	15°	ext	−0.22	0.06	−0.09	0.10	0.97	0.02	−67.21	8.43	35.26	6.50
		unl	−0.23	0.09	−0.02	0.08	0.97	0.03	−66.07	6.84	35.57	5.21
		fl	−0.25	0.04	−0.11	0.19	0.94	0.05	−60.54	6.19	36.15	4.40
	30°	ext	−0.23	0.11	−0.02	0.11	0.96	0.04	−69.03	7.38	34.80	7.78
		unl	−0.23	0.07	−0.04	0.08	0.97	0.02	−68.42	7.55	32.21	7.56
		fl	−0.27	0.09	−0.03	0.15	0.95	0.03	−63.19	7.67	33.58	6.95
ST	0°	ext	−0.31	0.03	−0.11	0.04	0.94	0.01	−74.17	4.72	30.61	3.90
		unl	−0.33	0.09	−0.09	0.03	0.93	0.03	−73.90	6.52	29.23	5.70
		fl	−0.37	0.07	−0.04	0.04	0.92	0.03	−63.60	6.78	32.38	5.95
	15°	ext	−0.27	0.07	−0.09	0.07	0.95	0.02	−76.17	8.44	33.39	4.41
		unl	−0.29	0.11	−0.06	0.08	0.95	0.04	−75.24	7.10	33.37	4.09
		fl	−0.32	0.08	−0.06	0.05	0.94	0.03	−68.44	6.84	31.13	3.38
	30°	ext	−0.25	0.08	−0.08	0.04	0.96	0.02	−78.31	5.79	32.57	6.59
		unl	−0.29	0.07	−0.08	0.04	0.95	0.02	−78.12	6.81	29.00	7.40
		fl	−0.38	0.11	−0.06	0.06	0.92	0.04	−71.85	7.21	29.02	5.80
GR	0°	ext	−0.25	0.09	0.10	0.08	0.96	0.02	−61.30	7.47	40.38	4.68
		unl	−0.31	0.10	0.11	0.05	0.94	0.04	−61.50	5.93	39.83	4.85
		fl	−0.34	0.08	0.14	0.05	0.93	0.03	−51.87	6.90	41.81	4.98
	15°	ext	−0.23	0.07	0.12	0.07	0.96	0.02	−63.12	11.34	43.18	6.04
		unl	−0.27	0.07	0.13	0.06	0.95	0.02	−62.50	9.03	43.53	4.42
		fl	−0.27	0.11	0.12	0.06	0.95	0.03	−57.21	8.45	42.90	3.82
	30°	ext	−0.26	0.07	0.12	0.08	0.95	0.03	−65.47	7.73	43.36	5.22
		unl	−0.27	0.04	0.08	0.08	0.96	0.01	−65.36	8.58	40.64	6.21
		fl	−0.37	0.12	0.12	0.11	0.91	0.04	−60.52	7.21	41.08	5.80
SR	0°	ext	−0.29	0.12	0.17	0.07	0.93	0.04	−60.61	7.25	42.68	5.24
		unl	−0.33	0.22	0.17	0.07	0.90	0.07	−59.84	8.57	42.22	5.40
		fl	−0.30	0.23	0.24	0.06	0.90	0.07	−50.00	7.85	44.25	5.68
	15°	ext	−0.18	0.16	0.21	0.06	0.95	0.05	−61.98	9.63	46.59	5.93
		unl	−0.21	0.10	0.19	0.05	0.95	0.03	−61.87	6.45	46.60	4.63
		fl	−0.33	0.19	0.17	0.07	0.91	0.06	−55.99	2.79	46.25	3.82
	30°	ext	−0.19	0.17	0.20	0.05	0.95	0.04	−64.77	7.83	46.33	5.08
		unl	−0.23	0.14	0.17	0.06	0.95	0.04	−65.21	7.18	43.76	5.88
		fl	−0.38	0.16	0.11	0.08	0.90	0.05	−58.72	5.71	44.29	5.23
BF	0°	ext	0.14	0.10	0.15	0.08	0.97	0.02	−52.85	3.27	−38.77	4.93
		unl	0.09	0.09	0.21	0.09	0.97	0.02	−52.84	4.15	−39.29	5.02
		fl	0.14	0.22	0.24	0.12	0.93	0.05	−49.37	4.29	−36.89	6.54
	15°	ext	0.12	0.15	0.15	0.10	0.97	0.03	−54.84	3.20	−37.88	6.63
		unl	0.04	0.13	0.16	0.15	0.97	0.03	−56.15	5.44	−37.42	3.99
		fl	0.05	0.13	0.23	0.14	0.95	0.05	−53.35	4.10	−35.76	5.74
	30°	ext	0.00	0.12	0.11	0.10	0.98	0.02	−56.75	4.37	−37.31	5.15
		unl	−0.03	0.10	0.14	0.10	0.98	0.02	−55.83	2.61	−38.04	5.69
		fl	−0.01	0.16	0.23	0.15	0.95	0.07	−53.28	3.25	−35.72	5.35

The location vector (in mm) is the point on the tendon at the level of the tibia plateau ($z = 10$ mm); the direction vector (in mm) is a unit vector that corresponds to the direction of the tendon. The origin of the system is located on the PT tendon 10 mm below the tibia plateau. PT = patella, SM = semimembranosus, ST = semitendinosus, GR = gracilis, SR = sartorius, BF = biceps femoris. 0°, 15° and 30° represent the conditions with 0°, 15° and 30° of knee joint flexion and ext, unl and fl are extension, unloaded and flexion conditions.

Table 3
Tendon angles in frontal and sagittal plane

Condition	PT		SM		ST		GR		SR		BF	
	Mean	SD	Mean	SD	Mean	SD	Mean	SD	Mean	SD	Mean	SD
Sagittal plane												
0°	32.0	6.0	−16.1	7.2	−19.6	4.3	−17.4	5.7	−18.7	11.6	7.3	8.6
15°	29.7	6.0	−13.6	4.0	−17.4	5.2	−15.2	5.0	−14.4	9.9	4.5	8.1
30°	27.2	5.3	−14.4	5.5	−18.1	6.0	−17.8	5.8	−15.9	10.5	−0.5	7.9
ext	27.3	4.1	−13.7	7.2	−16.3	3.8	−14.6	4.6	−13.4	9.3	4.9	8.0
unl	30.9	6.6	−14.7	5.0	−18.0	5.3	−16.8	4.3	−15.6	10.4	2.0	6.7
fl	30.6	6.6	−16.1	4.9	−21.2	5.6	−19.6	6.6	−20.5	11.7	3.9	11.3
Frontal plane												
0°	−15.9	7.1	7.0	8.3	5.1	2.8	−7.1	3.9	−11.9	4.7	−11.8	6.4
15°	−10.0	5.7	4.5	8.0	4.3	3.7	−7.4	3.7	−11.5	3.6	−10.5	7.8
30°	−8.3	5.4	2.1	6.8	4.5	3.0	−6.3	5.3	−9.8	4.3	−9.6	7.7
ext	−8.9	5.7	5.6	7.3	5.6	2.9	−6.8	4.5	−11.5	3.9	−7.9	5.6
unl	−15.1	7.4	3.0	5.7	4.8	3.1	−6.2	4.0	−10.8	3.8	−9.9	6.5
fl	−10.5	6.2	4.9	10.3	3.5	3.1	−7.7	4.7	−10.7	5.3	−14.1	8.3

Tendon angles in degrees are averaged (SD = standard deviation) over specific conditions (0°, 15° and 30° of knee flexion, ext = extension, unl = unloaded and fl = flexion conditions) in the sagittal plane (positive values = anterior, negative values = posterior direction of the tendon) and frontal plane (negative value = medial, positive value = lateral direction of the tendon).

Table 4
p-values of the ANOVA's

	PT	SM	ST	GR	SR	BF
Sagittal plane						
Knee angle	$0.001^{\#,3}$	0.252	0.087	0.366	0.228	$0.001^{\#,3}$
Ext/unl/fl	$0.005^{\#,4,5}$	0.246	$<0.001^{\#,5,6}$	$0.006^{\#,5}$	$0.001^{\#,5}$	0.338
Subject	$<0.001^{\#}$	$<0.001^{\#}$	$<0.001^{\#}$	$0.003^{\#}$	$<0.001^{\#}$	$<0.001^{\#}$
Knee angle*ext/unl/fl	0.552	0.950	0.266	0.478	0.179	0.932
Frontal plane						
Knee angle	$<0.001^{\#,1,3}$	$0.029^{\#,3}$	0.661	0.441	$0.028^{\#,3}$	0.096
Ext/unl/fl	$<0.001^{\#,4,6}$	0.300	$0.004^{\#,5}$	0.250	0.521	$<0.001^{\#,5,6}$
Subject	$<0.001^{\#}$	$<0.001^{\#}$	$<0.001^{\#}$	$<0.001^{\#}$	$<0.001^{\#}$	$<0.001^{\#}$
Knee angle*ext/unl/fl	0.168	0.505	0.117	0.299	$<0.001^{\#}$	0.753

PT = patella, SM = semimembranosus, ST = semitendinosus, GR = gracilis, SR = sartorius, BF = biceps femoris, ext = extension, unl = unloaded, fl = flexion, # = significant (p-value < 0.05), the numbers represent significant effects in the post-hoc test: 1 = 0° vs. 15°, 2 = 15° vs. 30°, 3 = 0° vs. 30°, 4 = ext vs. unl, 5 = fl vs. ext, 6 = fl vs. unl.

Table 5
The angle of the tendon line of action in the sagittal plane for individual subjects averaged over all conditions

Subject	*n*	PT		SM		ST		GR		SR		BF	
		Mean	SD	Mean	SD	Mean	SD	Mean	SD	Mean	SD	Mean	SD
1	9	33.4	4.3	−14.0	3.1	−17.5	2.7	−16.0	1.6	−8.6	6.2	3.1	6.0
2	6	24.1	4.8	−15.6	5.0	−22.1	6.7	−23.3	5.1	−20.9	9.5	6.3	10.1
3	9	31.7	6.5	−14.9	7.8	−13.3	2.7	−14.1	2.4	−8.5	9.7	1.3	4.1
4	9	29.6	5.2	−12.9	3.0	−25.4	2.7	−17.7	4.9	−4.9	2.8	14.9	6.5
5	9	35.5	5.8	−10.2	6.2	−17.8	6.2	−18.8	6.3	−19.5	11.6	2.3	10.1
6	5	25.8	1.8	−15.2	0.9	−14.0	3.3	−15.3	4.7	−25.8	7.2	2.6	8.8
7	9	24.2	4.1	−23.0	4.4	−17.1	3.3	−12.6	8.2	−25.8	4.9	−3.6	5.5
8	9	28.8	3.0	−13.0	3.1	−19.5	2.3	−19.2	2.8	−23.2	4.0	2.6	8.1
1–8	66	29.6	6.0	−14.8	5.8	−18.4	5.3	−17.0	5.6	−16.4	10.7	3.6	8.8

n = number of conditions, PT = patella, SM = semimembranosus, ST = semitendinosus, GR = gracilis, SR = sartorius, BF = biceps femoris, SD = standard deviation.

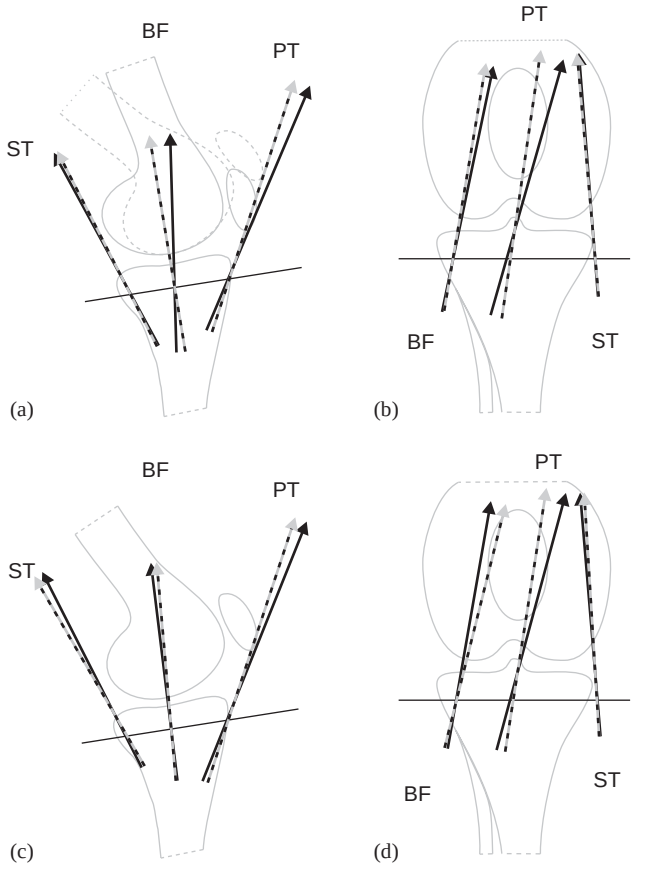

Fig. 5. Visualization of the directions of three tendons (BF = biceps femoris, PT = patella tendon, ST = semitendinosus) in two planes and four conditions, with schematic bone contours shown in gray. (a) Sagittal plane with 0° (black arrow) and 30° (gray dotted arrow) knee joint angle. (b) Frontal plane with 0° (black arrow) and 30° (gray dotted arrow) knee joint angle. (c) Sagittal plane with unloaded (black arrow) and extension (PT) or flexion (BF and ST) condition (gray dotted arrow). (d) Frontal plane with unloaded (black arrow) and extension (PT) or flexion (BF and ST) condition (gray dotted arrow).

All tendons in the MRI images were identified by the same author. The reliability was checked by repeated analysis of four random trials. The average differences in tendon angles between the first and second coloring were $0.1° \pm 1.5°$ (PT), $-1.7° \pm 1.9°$ (SM), $-0.2° \pm 1.0°$ (ST), $-1.4° \pm 3.0°$ (GR), $-1.9° \pm 3.5°$ (SR), and $-1.8° \pm 3.1°$ (BF) in the sagittal plane and $2.2° \pm 3.6°$ (PT), $-3.0° \pm 4.3°$ (SM), $0.8° \pm 1.3°$ (ST), $-0.6° \pm 2.4°$ (GR), $0.6° \pm 0.8°$ (SR), and $-0.1° \pm 2.3°$ (BF) in the frontal plane. The overall difference was $-1.2°$ ($\pm 2.4°$) in the sagittal plane and $0.0°$ ($\pm 2.9°$) in the frontal plane. The largest differences originated from series with movement artifacts.

4. Discussion

The main question of this study was whether muscle activation would influence tendon orientations. The load used in this study was relatively small (4.6 Nm). A larger load would be more comparable to loads during daily activities, but unfortunately, subjects were not able to maintain a larger force for the duration of the scanning. Nevertheless, this small force did have a significant effect on the orientation of the PT, ST, SR and BF tendons. The direction of the PT tendon was affected by muscle activation in both the sagittal and the frontal plane. In the sagittal plane, the difference between the unloaded and the extension effort was 3.6°. Although this difference may seem small, this does have a considerable effect on the shear component of the force exerted through this tendon. A tendon angle of 27.3° will lead to a shear force of 45.9 N when the force on the tendon is 100 N. The use of the 'unloaded' tendon angle instead of the 'extension' tendon angle will lead to an overestimation of the shear force of more than 10%. Therefore, even small differences in tendon angles are important when investigating shear forces. In the sagittal plane, two more tendons differed significantly between the loading conditions (ST and SR). Both tendons were orientated, respectively, 3.3° and 4.7° more posterior in the flexion trials compared to extension and unloaded trials.

No previous in vivo data have been published in which the effect of loading on muscle tendon directions was examined. There are two reasons that may cause the tendon orientation to change between loaded and unloaded conditions. The first is straightening of the tendon and the second is movement of the tibia relative to the femur. Imran et al. (2000) used a knee model that included relative tibia movement, but not tendon straightening. They predicted smaller effects of loading on the PT and hamstring tendon angles compared to the current study.

The results of the effect of knee joint angle are comparable to results found in literature. The direction of the PT tendon was affected by the knee joint angle in both the sagittal and the frontal plane. In the sagittal plane, the angle decreased by 4.7° when the knee was flexed from 0° to 30°. This is in agreement with Nisell et al. (1986) and Baltzopoulos (1995), who found respectively a decrease in PT angle of 6.5° and 5.7° in the same knee flexion range. As the knee is flexed from 0° to 15° and further on to 30°, the PT tendon was less medially directed in the frontal plane. This can be explained as part of the phenomenon of patella tracking (knee flexion leads to a more lateral position of the patella (Lin et al., 2003)) and 'screw-home mechanism' (external rotation of the tibia with respect to the femur near full extension (Piazza and Cavanagh, 2000)). Therefore, the angle of the PT tendon shifts laterally.

Anterior shear force on the tibia leads to strain on the anterior cruciate ligament (ACL) and a posterior shear force can counteract this anterior shear force. As one of the hamstring muscles, it is often assumed that the BF

exerts a posterior shear force when activated. However, this study showed that the BF tendon had an anterior orientation in knee joint angles of 0° and 15° and a neutral orientation in 30° of knee joint flexion. As a result, the BF tendon is not able to counteract anterior shear forces in knee joint angles of 0° and 15°, and it produces little to no shear force in knee joint angles of 30°. With a posterior tendon orientation, the other hamstring muscles (ST and SM) might be able to counteract anterior shear forces. However, between 0° and 30° of knee flexion, the anterior angle of the PT is much larger than the posterior angle of the hamstring (SM, ST and BF) tendons. The hamstring moment arm is smaller than the PT tendon moment arm (Kellis and Baltzopoulos, 1999), but the ratio of posterior shear force to flexion moment is smaller than the ratio of anterior shear force to extension moment of the quadriceps. Since additional activation (co-contraction) of the hamstrings during an extension implies an increase in quadriceps activation to maintain the same net moment, it seems unlikely that co-contraction reduces anterior shear forces in knee angles between 0° and 30°. It should be noted though that the conclusion whether hamstring posterior shear force is smaller or larger than the PT anterior shear force depends on the location of determining the tendon direction and the assumptions regarding the orientation of the tibia plateau. Tendons, cartilage and cortical bone are all black in T1-weighted images. Therefore, the insertion point could not reliably be determined. Additionally, there can be connective tissue around the tendon insertion, which can transmit forces, and the tendon direction may not be an adequate representation of force direction. At the level of the tibial plateau, the direction of the tendon is not interfered by other connective tissue. Regarding the orientation of the tibia plateau, assuming the cortical bone and cartilage layers were equally thick anterior and posterior of the medial tibia plateau, the plateau was oriented just below the cortical bone. It is interesting to note that Beynnon et al. (1995) measured no decrease in ACL strain in combined quadriceps and hamstrings contraction compared to isometric quadriceps contraction in 15° knee flexion. Different from what could be expected from this study, they did find a decrease in 30° knee flexion. This difference could be related to the assumptions regarding the tibia plateau orientation. Another possible explanation for the difference is that co-contraction increases joint compression and may thus increase the resistance of the joint surface against anterior tibia shear. This may reduce strain on the ACL. In addition, the data of the present study suggest that tendon angles are highly subject-specific. For instance, the ratio of PT to SM tendon angle varied from 0.95 in subject 7 to 0.29 in subject 5. The results of Beynnon et al. (1995) and the current study are based on a small number of subjects, and a between-group difference can thus not be excluded. The large inter-individual differences suggest that the usefulness of co-contraction as a strategy to counteract shear forces might depend on the subjects' anatomy. As a result, some subjects might run a higher risk of acquiring an ACL injury for instance. In ACL deficient subjects, Alkjaer et al. (2003) found differences in walking patterns between copers and non-copers. Tentatively, the differences between copers and non-copers can be ascribed to anatomical differences. Further research should be carried out to examine the range of the tendon angles and the possibility of an anatomically based explanation of the difference between copers and non-copers.

Acknowledgements

The authors would like to thank Dr. Leendert Blankevoort for his contribution in the early stages of the study. This study was supported by the Netherlands Organization for Scientific Research (NWO) and Stichting Anna Fonds. The support of the Canada Foundation for Innovation in acquiring the MR scanner used in this study is acknowledged. RF is an Alberta Heritage Foundation for Medicine Scholar and a Heart and Stroke Foundation of Canada Research Scholar.

References

Alkjaer, T., Simonsen, E.B., Jorgensen, U., Dyhre-Poulsen, P., 2003. Evaluation of the walking pattern in two types of patients with anterior cruciate ligament deficiency: copers and non-copers. European Journal of Applied Physiology and Occupational Physiology 89 (3–4), 301–308.

Baltzopoulos, V., 1995. A videofluoroscopy method for optical distortion correction and measurement of knee-joint kinematics. Clinical Biomechanics 10 (2), 85–92.

Beynnon, B.D., Fleming, B.C., Johnson, R.J., Nichols, C.E., Renstrom, P.A., Pope, M.H., 1995. Anterior cruciate ligament strain behavior during rehabilitation exercises in vivo. American Journal of Sports Medicine 23 (1), 24–34.

Blankevoort, L., Huiskes, R., 1996. Validation of a three-dimensional model of the knee. Journal of Biomechanics 29 (7), 955–961.

Brand, R.A., Crowninshield, R.D., Wittstock, C.E., Pedersen, D.R., Clark, C.R., van Krieken, F.M., 1982. A model of lower extremity muscular anatomy. Journal of Biomechanical Engineering 104 (4), 304–310.

Buford Jr., W.L., Ivey Jr., F.M., Malone, J.D., Patterson, R.M., Peare, G.L., Nguyen, D.K., Stewart, A.A., 1997. Muscle balance at the knee—moment arms for the normal knee and the ACL minus knee. IEEE Transactions on Rehabilitation Engineering 5 (4), 367–379.

Crisco, J.J., McGovern, R.D., 1998. Efficient calculation of mass moments of inertia for segmented homogeneous three-dimensional objects. Journal of Biomechanics 31 (1), 97–101.

El-Dieb, A., Yu, J.S., Huang, G.S., Farooki, S., 2002. Pathologic conditions of the ligaments and tendons of the knee. Radiologic Clinics of North America 40 (5), 1061–1079.

Herzog, W., Read, L.J., 1993. Lines of action and moment arms of the major force-carrying structures crossing the human knee joint. Journal of Anatomy 182 (Pt 2), 213–230.

Imran, A., Huss, R.A., Holstein, H., O'Connor, J.J., 2000. The variation in the orientations and moment arms of the knee extensor and flexor muscle tendons with increasing muscle force: a mathematical analysis. Proceedings of the Institution of Mechanical Engineers Part H—Journal of Engineering in Medicine 214 (H3), 277–286.

Jaramillo, D., Laor, T., Mulkern, R.V., 1994. Comparison between fast spin-echo and conventional spin-echo imaging of normal and abnormal musculoskeletal structures in children and young adults. Investigative Radiology 29 (9), 803–811.

Kellis, E., Baltzopoulos, V., 1999. In vivo determination of the patella tendon and hamstrings moment arms in adult males using videofluoroscopy during submaximal knee extension and flexion. Clinical Biomechanics 14 (2), 118–124.

Koolstra, J.H., van Eijden, T.M., Weijs, W.A., 1989. An iterative procedure to estimate muscle lines of action in vivo. Journal of Biomechanics 22 (8–9), 911–920.

Lin, F., Makhsous, M., Chang, A.H., Hendrix, R.W., Zhang, L.Q., 2003. In vivo and noninvasive six degrees of freedom patellar tracking during voluntary knee movement. Clinical Biomechanics 18 (5), 401–409.

Lloyd, D.G., Buchanan, T.S., 1996. A model of load sharing between muscles and soft tissues at the human knee during static tasks. Journal of Biomechanical Engineering 118 (3), 367–376.

Major, N.M., Helms, C.A., 2002. MR imaging of the knee: findings in asymptomatic collegiate basketball players. American Journal of Roentgenology (AJR) 179 (3), 641–644.

Munshi, M., Pretterklieber, M.L., Kwak, S., Antonio, G.E., Trudell, D.J., Resnick, D., 2003. MR imaging, MR arthrography, and specimen correlation of the posterolateral corner of the knee: an anatomic study. American Journal of Roentgenology (AJR) 180 (4), 1095–1101.

Nisell, R., Nemeth, G., Ohlsen, H., 1986. Joint forces in extension of the knee. Analysis of a mechanical model. Acta Orthopaedica Scandinavica 57 (1), 41–46.

O'Connor, J.J., 1993. Can muscle co-contraction protect knee ligaments after injury or repair? Journal of Bone and Joint Surgery-British Volume 75 (1), 41–48.

Piazza, S.J., Cavanagh, P.R., 2000. Measurement of the screw-home motion of the knee is sensitive to errors in axis alignment. Journal of Biomechanics 33 (8), 1029–1034.

Ronsky, J. L., 1994. In-vivo quantification of patellofemoral joint contact characteristics. Ph.D. dissertation Thesis, University of Calgary, Calgary, Canada.

Shelburne, K.B., Pandy, M.G., 1997. A musculoskeletal model of the knee for evaluating ligament forces during isometric contractions. Journal of Biomechanics 30 (2), 163–176.

Spoor, C.W., van Leeuwen, J.L., 1992. Knee muscle moment arms from MRI and from tendon travel. Journal of Biomechanics 25 (2), 201–206.

Wretenberg, P., Nemeth, G., Lamontagne, M., Lundin, B., 1996. Passive knee muscle moment arms measured in vivo with MRI. Clinical Biomechanics 11 (8), 439–446.

Zavatsky, A.B., O'Connor, J.J., 1992. A model of human knee ligaments in the sagittal plane. Part 1: Response to passive flexion. Proceedings of the Institution of Mechanical Engineers Part H—Journal of Engineering in Medicine 206 (3), 125–134.